

Twist Mode in Spherical Alkali Metal Clusters

V. O. Nesterenko,^{1,2} J. R. Marinelli,¹ F. F. de Souza Cruz,¹ W. Kleinig,^{2,3} and P.-G. Reinhard⁴

¹*Departamento de Física, Universidade Federal de Santa Catarina, Florianópolis, SC 88040-900, Brazil*

²*Bogoliubov Laboratory of Theoretical Physics, Joint Institute for Nuclear Research, Dubna, Moscow region, 141980, Russia*

³*Technische Universität Dresden, Institut für Analysis, D-01062 Dresden, Germany*

⁴*Institut für Theoretische Physik, Universität Erlangen, D-91058 Erlangen, Germany*

(Received 17 April 2000)

A remarkable orbital quadrupole magnetic resonance, so-called twist mode, is predicted in alkali metal clusters where it is represented by $I^\pi = 2^-$ low-energy excitations of valence electrons with strong $M2$ transitions to the ground state. We treat the twist by both macroscopic and microscopic ways. In the latter case, the shell structure of clusters is fully exploited, which is crucial for the considered size region ($8 \leq N_e \leq 1314$). The energy-weighted sum rule is derived for the pseudo-Hamiltonian. In medium and heavy spherical clusters, the twist dominates over its spin-dipole counterpart and becomes the most strong multipole magnetic mode.

PACS numbers: 36.40.Cg, 36.40.Gk, 36.40.Vz, 36.40.Wa

Orbital magnetism in atomic clusters is a subject of special interest. Clusters may contain many atoms and, therefore, single-particle orbital moments of valence electrons can reach very big values. This results in huge orbital effects, for example, in strong orbital magnetic resonances. These resonances are of a general character and exist in different finite Fermi systems (nuclei, atomic clusters, etc.). $M1$ scissor mode in deformed systems [1–4] and $M2$ twist mode in systems of arbitrary shape [5–10] are the most famous examples. They have been observed in atomic nuclei (see, e.g., [2,9]) but not yet in clusters. The scissors mode has been already predicted in clusters [3,4]. In the present paper we will discuss properties of the twist mode in this system.

By definition, the twist is the quadrupole torsional vibration mode of an elastic globe [5]. It is generated by the operator $\hat{T} = e^{-i\alpha z l_z} = e^{\alpha \vec{u} \cdot \vec{\nabla}}$ with the velocity field $\vec{u} = (yz, -xz, 0)$ [5,6]. The mode is viewed macroscopically (see Fig. 1) as small-amplitude rotationlike oscillations of different layers of a system against each other with a rotational angle proportional to z (projection to the axis of rotation). The restoring force of the twist is determined by the quadrupole distortions of the Fermi surface in the *momentum* space. So, the twist represents transverse magnetic quadrupole oscillations of an *elastic* medium, provided by variations of the kinetic-energy density. The twist is a general feature of any three-dimensional finite Fermi system which demonstrates an elastic behavior. Atomic nuclei [6–9] and clusters [10] are the most typical examples. Unlike the $M1$ scissor mode which has the similar quantum origin but can exist only in deformed systems, the twist manifests itself in Fermi systems of any shape, spherical and deformed.

Expressions for the twist energy and $M2$ strength, obtained within the elastodynamical models [6,8] for atomic nuclei, can be reformulated for clusters as

$$\omega = 17 \text{ eV } \text{Å}^2 r_s^{-2} N_e^{-1/3}, \quad B(M2) = 0.52 r_s^2 N_e^2 \mu_b^2, \quad (1)$$

where $B(M2)$ is the probability of an $M2$ transition from the ground state to a 2^- twist state, r_s is the Wigner-Seitz radius, and N_e is the number of valence electrons. We will show that expressions (1) provide good qualitative agreement with microscopic results. However, elastodynamical models do not access the shell structure of nanoparticles and so cannot clarify the microscopic origin of the twist. Moreover, these models are questionable for small systems. In this paper we will present, for the first time, a microscopic analysis of the twist, fully embracing shell effects. Both small and heavy clusters will be covered.

The operator for $M2$ transition [11], $\hat{F}(M2, \mu) = \mu_b \sqrt{10} r [g_s \{Y_1 \hat{s}\}_{2\mu} + \frac{2}{3} g_l \{Y_1 \hat{l}\}_{2\mu}]$, is a sum of spin and orbital components with $g_s = 2$ and $g_l = 1$. The external field generating the twist, $z l_z \propto r(Y_{10} l_z)$, is a part of the orbital component with $\mu = 0$. So, it is natural to consider the twist as a part of the orbital $M2$ resonance. Since both are of a similar nature, we will call the whole orbital $M2$ resonance also a twist.

In spherical systems, only the spin-dipole channel delivers the residual interactions for 2^- excitations. Investigations [7,12] have shown that twist in spherical atomic

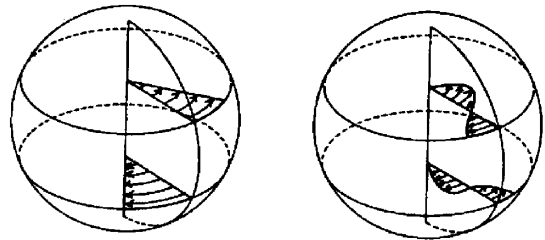


FIG. 1. Nodeless (left) and one-node (right) branches of twist mode [6].

nuclei depends only weakly on this residual interaction and the remaining dependence is caused mainly by the spin-orbit coupling. The influence of the residual interaction should then be even smaller for metal clusters where the spin-orbit coupling is negligible. Thus, we can deal with a simple particle-hole ($1p-1h$) picture. Also, we will confine our consideration to the spherical jellium model which is compulsory for analysis of large systems. These two approximations are appropriate for the present purpose of a first survey of the twist mode. At the side of the mean field Hamiltonian, we take into account local as well as nonlocal effects which are caused by the ionic pseudopotential. For Na and K clusters, we calculate the Kohn-Sham single-particle scheme within the approach [13] which properly treats the local effects. For Li clusters, the pseudo-Hamiltonian [14],

$$H_0 = -\frac{\hbar^2}{2m_e} \vec{\nabla} \cdot [1 + \alpha(r)] \vec{\nabla} + \vec{L} \cdot \beta(r) \vec{L} + u(r) + W(r), \quad (2)$$

with the parametrization [15] is used. The local ionic contribution is carried in $u(r)$, and nonlocal effects lead to the effective mass $m^*(r) = m_e/[1 + \alpha(r)]$ and the orbital term $\propto \beta(r)$. Coulomb and exchange-correlation potentials are represented by $W(r)$.

Results of our studies are exhibited in Figs. 2–4 and Table I. In Fig. 2 the orbital $M2$ strength, $B(M2) =$

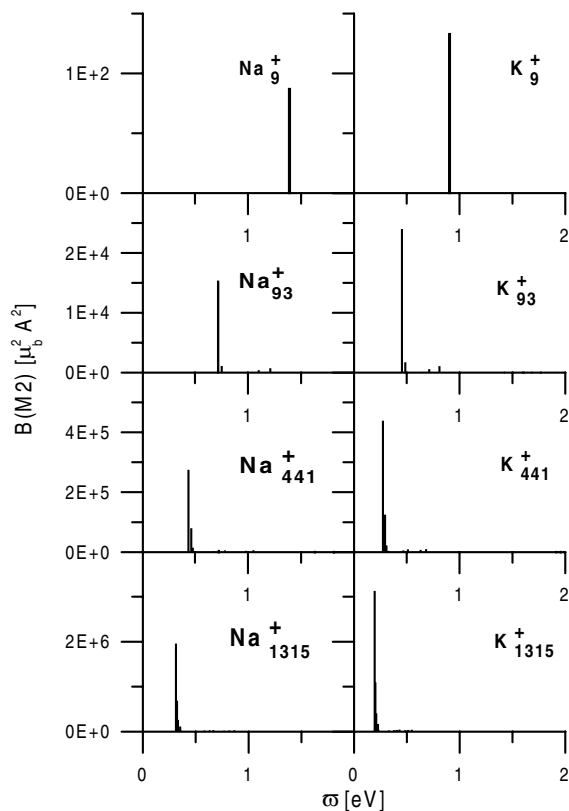


FIG. 2. The distribution of $M2$ strength in spherical Na (left) and K (right) clusters of different sizes, as indicated.

$\langle i | \hat{F}(M2) | 0 \rangle^2$, is presented for light, medium, and heavy spherical Na and K clusters [i represents $(1p-1h)_2$ -states]. Only the orbital part of the $M2$ transition operator is used. Figure 2 shows that dominant twist strength is concentrated in the one $1p-1h$ peak with the lowest energy. This relation persists independent of N because both the twist mode and other relevant $1p-1h$ excitations follow a trend $\propto N_e^{-1/3}$ (see also Fig. 4). The degree of concentration, however, changes with N . The twist peak exhausts 100%, 80%, and 60% of the total $M2$ strength in Na_9^+ , Na_{93}^+ , and Na_{1315}^+ , respectively. It corresponds to the nodeless branch of the twist mode (see Fig. 1, left side). The nature of the peak is clarified in Fig. 3. It represents $n, l \rightarrow n, l + 1$ transition between single-particle levels with the node number $n = 1$ and maximal orbital moments l . The levels belong to the last occupied and the first empty shells. As a result, the twist can serve as a valuable source of information about (i) single-particle levels with maximal orbital momenta near the Fermi surface and (ii) the energy gap, ΔE_{sh} , between the Fermi and next empty shells.

In large clusters weaker peaks also contribute to the twist resonance. As a rule, they represent $n, l \rightarrow n, l + 1$ transitions with $n = 2, 3, \dots$ and lower orbital moments. Following our analysis of the velocity field, these peaks also contribute mainly to the nodeless twist branch (Fig. 1, left side). Their contribution grows with increasing cluster size. They come energetically closer to the dominant peak (see Fig. 2) such that they may not be easily distinguishable experimentally. Other twist branches (see, e.g., the right side of Fig. 1) carry only a small fraction of the total strength and lie at higher energies.

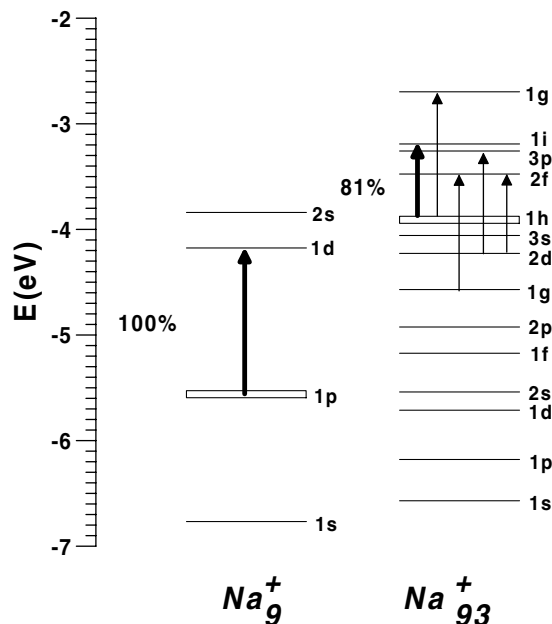


FIG. 3. Single-particle levels and $M2$ $1p-1h$ transitions in Na_9^+ and Na_{93}^+ . The Fermi levels are marked by the double line. For the main transitions (bold arrows), the contributions to the complete strength $B(M2)$ are given.

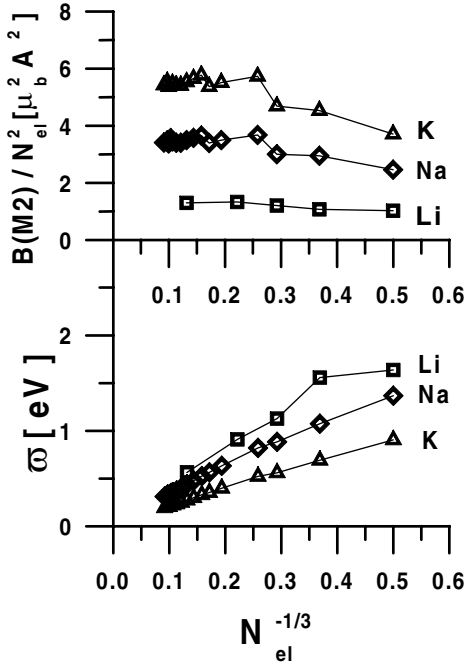


FIG. 4. The strength normalized by N_e^2 (upper panel) and averaged energy (lower panel) of the twist resonance in K, Na, and Li clusters. The trends $B(M2) \propto N_e^2$ and $\bar{\omega} \propto N_e^{-1/3}$ are distinctive.

Figure 2 demonstrates the similarity of the twist in Na and K clusters. A much similar pattern appears for Li. However, there are also distinctive differences in twist energies and strength. These values are compared in Fig. 4. K, Na, and Li are distinguished by Wigner-Seitz radii [in atomic units, $r_s(\text{K}) = 5$, $r_s(\text{Na}) = 3.96$, and $r_s(\text{Li}) = 3.25$, respectively] and by the different influence of the ionic structure. Figure 4 shows the following trends: (i) The denser the metal, the higher the twist energy. This can be explained by the fact that the smaller the r_s , the deeper the corresponding single-particle potential [16]. In Li clusters the potential is most deep and, therefore, has the largest energy gap ΔE_{sh} between neighboring quantum shells. Being close to ΔE_{sh} , the twist energy should increase from K to Li. (ii) In all the size regions the twist mode resides far below the Mie dipole plasmon and, at the same time, it stays still far above typical ionic

TABLE I. Orbital energy-weighted sum rule S_l (in units $\mu_b^2 \text{Å}^2 \text{eV}$) and ratio $R = S_l/S_s$ for Na and Li spherical clusters in the energy interval 0–6 eV (95%–99% of the sum rules are exhausted in the interval 0–2 eV). Values R are equal for K, Na, and Li clusters of the same size.

N_e	S_l		R
	K, Na	Li	K, Na, Li
8	1.21×10^2	1.08×10^2	0.33
20	7.28×10^2	6.42×10^2	0.80
40	2.55×10^3	2.23×10^3	1.40
92	1.35×10^4	1.15×10^4	3.21
440	2.01×10^5	1.67×10^5	9.72

vibrations ($\omega \approx 50$ meV), which both help for an experimental discrimination. The heavier the cluster, the smaller the energy gap ΔE_{sh} and, therefore, the twist energy. Figure 4 demonstrates the energy fall $\propto N_e^{-1/3}$. It is worth noting that such dependence of twist energy takes place in both atomic clusters and nuclei. (iii) The denser the metal, the smaller the resonance strength. As is shown below, the energy-weighted sum rule S_l keeps the same value for K, Na, and Li clusters of a given size (if one neglects the ionic structure effects). So, the increase in the excitation energy has to result in the decrease of the strength. In Li clusters the strength is additionally suppressed due to the effective mass, $m^*/m_e \sim 1.2$. (iv) $B(M2)$ grows as N_e^2 (see upper part of Fig. 4).

All the trends discussed above are supported by the elastodynamical results (1). However, the quantitative agreement is less perfect. Equations (1) considerably overestimate both twist energy and strength (up to 80% and 30% in light and heavy clusters, respectively). That is not so surprising because we find that the twist mode is dominated by the shell structure while the collective model averages over shells.

The attractive feature of the orbital $M2$ mode is that its total strength can be estimated in a simple fashion by the energy-weighted sum rule as

$$\begin{aligned}
 S &= \sum_i \omega_i |\langle i | \hat{F}(M2) | 0 \rangle|^2 \\
 &\approx \frac{1}{2} \sum_{\mu=-2}^2 \langle 0 | [\hat{F}(M2\mu), [H_0, \hat{F}(M2\mu)]] | 0 \rangle = S_s + S_l,
 \end{aligned} \tag{3}$$

where

$$\begin{aligned}
 S_s &= \frac{75\hbar^2}{2\pi m_e} \sum_{n,l_i}^{\text{occ}} (2l_i + 1) \int (1 + \alpha + 8r^2\beta) \rho_{n,l_i} dr, \\
 S_l &= \frac{25\hbar^2}{3\pi m_e} \sum_{n,l_i}^{\text{occ}} (2l_i^3 + 3l_i^2 + l_i) \\
 &\quad \times \int \left(1 + \alpha + \frac{8}{5} r^2\beta\right) \rho_{n,l_i} dr
 \end{aligned} \tag{4}$$

are contribution of the spin and orbital parts of the transition operator $\hat{F}(M2)$. In Eq. (3) the sum runs over all $(1p-1h)_2-$ states. In Eqs. (4), $\alpha(r)$ and $\beta(r)$ are the functions responsible for the nonlocal effects in the pseudo-Hamiltonian (2), $\rho_{n,l_i} = [rR_{n,l_i}(r)]^2$, and $R_{nl}(r)$ is the radial wave function of the single-particle state nl . In Eqs. (4), the sum runs over all occupied single-particle levels. The spin-orbit coupling is neglected in the calculations, but it would not contribute directly to S_l anyway. Without the spin-orbit coupling, the spin-dipole residual two-body interaction also does not contribute to S_l . The calculations show that, even for Li clusters, one may safely neglect the spin-orbit correction β because it contributes less than 0.1%. The influence of the correction α is strong

in Li: we have $m_e^*/m_e \sim 1.2$ [17] and so this correction decreases S_I by a factor of $\sim 4/5$.

If one neglects the nonlocal corrections (which is justified for Na and K clusters [14,17]), then the radial integrals in Eqs. (4) are just 1, and both S_s and S_I become very simple and even *model independent* (the similar sum rules have been derived for the twist in atomic nuclei [7] and spin-dipole excitations in clusters [18]). This is evident for S_s where $2 \sum_{n,l}^{\text{occ}} (2l+1) = N_e$. As for S_I , one should mention that different models predict, as a rule, the same sequence of occupied levels in spherical clusters, at least for light and medium sizes. Finally, it is worth emphasizing that (i) the calculation of S_I is extremely simple: it is enough to know the orbital moments l of occupied single-particle levels; (ii) both S_s and S_I values are equal for clusters of a given size but of different metals (K, Na), which agrees with Eqs. (1).

The twist part, $\mu_b \sqrt{80/27} r Y_{10} l_z$, of the transition operator $\hat{F}(M2)$ gives exactly 4/9 of the complete S_I values. Following Fig. 1, the twist represents the oscillations in equatorial planes. The total orbital $M2$ resonance takes also into account the meridian oscillations.

Results presented in Table I show that the orbital $M2$ energy-weighted strength *dominates* over the spin one already in clusters with $N_e = 40$. Starting with $N_e = 92$, the orbital contribution becomes overwhelming and, already for $N_e = 440$, demonstrates a huge value of $2 \times 10^5 \mu_b^2 \text{ \AA}^2 \text{ eV}$. Since the long-wave $M1$ response, both spin and orbital, is forbidden in spherical clusters (indeed, both spin and orbital $1p-1h$ matrix elements of $M1$ transition are proportional to the radial integral $\int R_{n_1 l_1}(r) R_{n_2 l_2} r^2 dr = \delta_{n_1 l_1, n_2 l_2}$ which is zero in the non-diagonal case due to orthonormalization condition), the twist starting with medium sizes becomes the *strongest* multipole magnetic mode. This fact emphasizes its fundamental character.

Our calculations indicate that twist mode cannot be detected in photoabsorption spectra since it is masked by low-energy $E1$ excitations. These excitations are much weaker than the dipole plasmon but, nevertheless, strong enough to mask the twist. The inelastic scattering of polarized optical photons (resonant Raman scattering) seems to be more appropriate to observe the twist, though any conclusions about perspectives of these reactions still requires a careful analysis of the competition between $E1$, $E2$, and $M2$ modes. The Raman scattering can separate electric and magnetic modes due to the polarization selection rules. Clusters with about 10^4 atoms seem to be optimal. In such clusters, the twist strength reaches impressive values and, at the same time, is strongly concentrated at a very narrow low-energy interval (which remains still well separated from ionic vibrations). Our estimations show that in heavy clusters, in spite of a dense spectrum, the twist exists and carries the spectroscopic information mentioned above.

In summary, the $M2$ orbital resonance and its important part, the twist mode, have been investigated in spherical alkali metal clusters. The macroscopic treatment of the twist exhibits this mode as a general feature of any finite three-dimensional Fermi system and provides a pertinent description of the basic trends. However, it is not delivering a quantitative agreement. The microscopic treatment, including the novel energy-weighted sum rules, clarifies the main properties of twist $1p-1h$ $M2$ response. The resonance is mainly exhausted, first of all in clusters of a moderate size, by one $1p-1h$ $M2$ transition connecting the Fermi and next empty quantum shell, namely, their levels with maximal orbital moments. As a result, the twist can provide valuable information about the single-particle scheme. Twist energy and strength evolve with a cluster size as $\omega \sim N_e^{-1/3}$ and $B(M2) \sim N_e^2$. In heavy clusters an impressive $M2$ strength can be reached. The twist *dominates* in the low-energy region over its spin-dipole counterpart already in clusters of a moderate size and finally becomes the strongest magnetic multipole mode. We hope that the fundamental significance of the twist for orbital magnetism in spherical clusters will encourage experimentalists to look for proper ways for its observation.

We thank E. Duval and N. Lo Iudice for useful discussions and L. Serra for presenting single-particle schemes for Li clusters. The work was partly supported (V. O. N.) by RFBR Grant No. 00-02-17194.

-
- [1] N. Lo Iudice and F. Palumbo, Phys. Rev. Lett. **41**, 1532 (1978).
 - [2] N. Pietralla *et al.*, Phys. Rev. C **58**, 184 (1998).
 - [3] E. Lipparini and S. Stringari, Phys. Rev. Lett. **63**, 570 (1989).
 - [4] V. O. Nesterenko *et al.*, Phys. Rev. Lett. **83**, 57 (1999).
 - [5] H. Lamb, Proc. London Math. Soc. **13**, 187 (1882).
 - [6] G. Holzward and G. Ekardt, Z. Phys. A **283**, 1532 (1978); Nucl. Phys. **A325**, 1 (1979).
 - [7] B. Schwesinger, Phys. Rev. C **29**, 1475 (1984).
 - [8] S. I. Bastrukov and I. V. Molodtsova, Phys. Part. Nucl. **26**, 180 (1995).
 - [9] P. von Neumann-Cosel *et al.*, Phys. Rev. Lett. **82**, 1105 (1999).
 - [10] S. I. Bastrukov, Phys. Rev. E **49**, 3166 (1994).
 - [11] J. M. Blatt and V. F. Weisskopf, *Theoretical Nuclear Physics* (Wiley, New York, 1952).
 - [12] J. Kvasil *et al.*, Phys. Rev. C **58**, 209 (1998).
 - [13] B. Montag, P.-G. Reinhard, and J. Meyer, Z. Phys. D **32**, 125 (1994).
 - [14] L. Serra *et al.*, Phys. Rev. B **48**, 14 708 (1993).
 - [15] J. Lermé, Phys. Rev. B **54**, 14 158 (1996).
 - [16] P.-G. Reinhard, O. Genzken, and M. Brack, Ann. Phys. (Leipzig) **5**, 576 (1996).
 - [17] W. Kleinig *et al.*, Eur. Phys. J. D **4**, 343 (1998).
 - [18] L. Serra and E. Lipparini, Z. Phys. D **42**, 227 (1997).